CVGIP: IMAGE UNDERSTANDING
Vol. 57, No. 3, May, pp. 359–372, 1993

A Review of Recent Texture Segmentation and Feature Extraction Techniques

TODD R. REED

Center for Image Processing and Integrated Computing, and Department of Electrical and Computer Engineering, University of California, Davis, California 95616

AND

J. M. HANS DU BUF

Signal Processing Laboratory, Swiss Federal Institute of Technology, EPFL - Ecublens, CH-1015 Lausanne, Switzerland

Received October 24, 1991; revised July 24, 1992

The area of texture segmentation has undergone tremendous growth in recent years. There has been a great deal of activity both in the refinement of previously known approaches and in the development of completely new techniques. Although a wide variety of methodologies have been applied to this problem, there is a particularly strong concentration in the development of feature-based approaches and on the search for appropriate texture features. In this paper, we present a survey of current texture segmentation and feature extraction methods. Our emphasis is on techniques developed since 1980, particularly those with promise for unsupervised applications. © 1993 Academic Press, Inc.

1. INTRODUCTION

Texture segmentation has been attempted in numerous ways. It is often obtained by adopting the independent subprocesses of texture feature extraction, feature selection or reduction if the number of features is too large, followed by a segmentation algorithm. Feature extraction methods may be categorized, roughly, as feature-based, model-based, and structural. In feature-based methods, some characteristic or characteristics of textures are chosen and regions in which these characteristics are relatively constant (or the boundaries between the regions) are sought. Model-based methods hypothesize underlying processes for textures and segment using certain parameters of these processes. Since model parameters are used as texture features, model-based methods could be considered a subclass of feature-based methods. Finally, structural methods seek to partition images under the assumption that the textures in the image have detectable primitive elements, arranged according to placement rules.

The main purpose of texture feature extraction is to map differences in spatial structures, either stochastic or geometric, into differences in gray value. Segmentation methods then analyse the feature space in order to extract homogeneous regions. Segmentation methods are often classified as region-based, boundary-based, or as a hybrid of the two. Although membership in one of the above groups does not exclude membership in another and there are methods that do not fall neatly into any of these categories, we will use the above classes to give structure to the discussion that follows. We note that boundary-based methods often analyse feature statistics within adjacent windows, in the same way that region-based methods do. However, the main difference between these approaches is that region-based methods seek feature homogeneity, while boundary-based methods attempt to detect feature inhomogeneities.

Due to the large amount of activity in this field, to treat all published techniques would be an extremely difficult task. As a result, detailed discussion will be limited to methods with potential for unsupervised texture segmentation. In this way, we hope to complement existing surveys, e.g., [1–5].

2. FEATURE-BASED METHODS

In discussing feature-based texture segmentation methods, it is convenient to consider separately those methods that are interesting primarily due to unique features and those which use unique methods of performing the segmentation. Refining these categories further, many features may be considered as derived from operators, from statistical tests, or from examination of the image in a transform domain.

1049-9660/93 $5.00

2.1. Methods Using Unique Features

2.1.1. *Operator-Based Features*

A first example of the derivation of features using operators is the set of "texture energy measures" formulated by Laws in [6]. Small (e.g., 5 × 5), center-weighted filter masks are convolved with the image to be segmented. Statistics, such as the variance, are computed within a window about each pixel in the resulting (filtered) images. The values of the statistics are assigned as features to the corresponding pixel in the original image. It is noted that Laws' basic filter functions, with their characteristic oscillations, have a striking similarity to Gabor functions (as to wavelets, Hermite polynomials, prolate spheroidal functions, etc.; see Section 5). However, since the filter masks are relatively small, only the high-frequency content of textures can be analysed.

In [7], Conners, Trivedi, and Harlow derive texture operators from the co-occurrence matrices used by the spatial gray level dependence method [8]. From each matrix, six measures (inertia, cluster shade, cluster prominence, local homogeneity, energy, and entropy) are calculated for use as features. The classes into which textures are segmented were selected to correspond to the Defense Mapping Agency's Mapping, Charting, and Geodesy tangible features.

A simple operator for fast discrimination between textured and uniform regions is proposed by Dinstein *et al.* in [9]. The pixel in the output image corresponding to the center pixel of each K × K window in the original image is set to the difference between the maximum and minimum gray level occurring in the window. The value returned by the operator is high for textured regions and low for homogeneous ones, allowing discrimination between these regions. An algorithm for fast application of the operator is shown. This operator also acts as an edge detector between uniform regions with different gray values.

A method similar to that proposed by Laws was introduced by Unser in [10], who examined different transformations. For example, in a first pass the input image is convolved with four 2 × 2 Hadamard masks. These masks measure the local average, as well as estimate the local derivatives in horizontal, vertical, and oblique directions. In a second pass local statistics, such as the variance, are gathered.

Another method similar to that of Laws is described by Wang, Hanson, and Riseman in [11]. Rather than the "edge-like," "high-frequency spot-like," etc., masks used in [6], a set of simple (vertical, horizontal, diagonal, and anti-diagonal) masks are applied. A comparative experiment is performed using these simple masks and four high order masks proposed by Laws. Results as good as, or better than, those achieved using the Laws masks are reported.

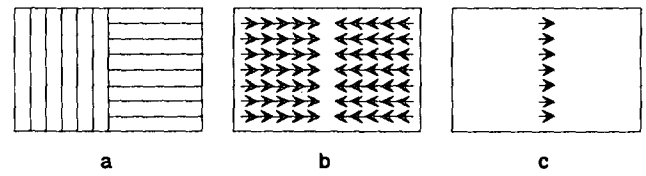

FIG. 1. An example of Granlund's method: (a) The original image; (b) The result of the first application of the operator; (c) The result of the second application of the operator.

Finally, an operator-based technique that has been considered for unsupervised texture segmentation is described by Granlund in [12]. The operator proposed, called the "general operator," measures the direction and magnitude of gray scale change in the operator field. This is accomplished by applying a set of orientation sensitive masks to the image and by selecting as the operator output the magnitude and orientation from the mask with the largest response. Texture segmentation is achieved by applying this operator to a previously transformed image. As shown in the example of Fig. 1, the first application of the operator yields the direction and magnitude of maximum change for the image textures, while the second gives the boundary between texture fields. Wermser and Lissel [13] have compared Granlund's method with that of Abele [14] (a statistical method described in the next section) and the method of Chen and Pavlidis [15] (co-occurrence matrices used with a split-and-merge algorithm) for unsupervised texture segmentation. It was found that good results were obtained most often with textures having strong differences in direction. Difficulties were encountered in the presence of noise and when textures were irregular.

More sophisticated operators have been defined by Knutsson and Granlund in [16]. These operators, measuring the dominant local orientation or the dominant local frequency as well as their associated certainties, are based on combining the outputs of quadrature filter pairs with polar-separable modulation transfer functions. This concept has been refined by Bigun in [17]. The latter author obtains a more complete texture description by applying the dominant local orientation estimation at different frequency scales using a Laplacian pyramid. This anisotropic information is combined with isotropic information, which is mediated by the power as estimated in octave frequency bands.

2.1.2. *Statistically Based Features*

One of the first methods used in texture segmentation, and still a major one, is the spatial gray level dependence

method. In [8], Haralick, Shanmugam, and Dinstein define the gray-tone spatial-dependence matrix as follows. Given an image $f(x, y)$ with a set of N_g discrete gray levels, define the matrix $P(i, j, d, \theta)$ such that the (i, j)th entry is the number of times that

$$f(x_1, y_1) = i$$

and

$$f(x_2, y_2) = j,$$

where

$$(x_2, y_2) = (x_1, y_1) + (d\cos\theta, d\sin\theta). \quad (1)$$

This yields a matrix of dimension equal to the number of gray levels in the image, for each distance and orientation (d, θ). Examples of features extracted from these matrices are *angular second moment*

$$E(d, \theta) = \sum_{i=1}^{N_g}\sum_{j=1}^{N_g}\left[\frac{P(i, j, d, \theta)}{R(d, \theta)}\right]^2 \quad (2)$$

and *entropy*

$$H(d, \theta) = -\sum_{i=1}^{N_g}\sum_{j=1}^{N_g}\frac{P(i, j, d, \theta)}{R(d, \theta)}\log\frac{P(i, j, d, \theta)}{R(d, \theta)}, \quad (3)$$

where $R(d, \theta)$ is the number of neighboring resolution cell pairs. This method has proven quite successful. However, many of the texture features that are derived using this method have little correlation with features visible to the human eye.

In contrast, Tamura, Mori, and Yamawaki made an attempt at defining a set of visually relevant texture features in [18]. This set includes coarseness, contrast, directionality, line-likeness, regularity, and roughness. Most of these measures showed a reasonable correspondence to the results of psychophysical tests, in which human subjects ranked Brodatz textures with respect to their impression of these subjective attributes.

A method using both statistical and structural features that has been proposed for unsupervised applications is described by Abele in [14]. Features for segmentation are selected from a large set of features associated with texture primitives (Table 1). Here, texture primitives are connected subregions with approximately constant intensity. The selection is performed by a space-invariant, nonlinear operation, the purpose of which is to reduce the distance between primitives in the same class, while increasing the distance between different classes. The distance function between primitives Q_i and Q_j is defined as

$$D_{ij} = \begin{cases} \frac{1}{n_{ij}} \cdot \mid (f_i - f_j)t_{ij} \mid + d_{ij} & \text{if } n_{ij} \neq 0 \\ z + d_{ij} & \text{if } n_{ij} = 0, \end{cases} \quad (4)$$

where

f_i, f_j are the portions of the feature vectors for Q_i and Q_j that are primitive related,

$t_{ij} = (s_i'.\text{AND}.s_j')$,

$n_{ij} = t_{ij}^T t_{ij}$ = number of features set to one in s_i and s_j,

d_{ij} = the spatial distance between primitives' gravity centers,

$$s_i(k) = \begin{cases} 1 & \text{if } \Sigma_j C_{ij}(k) > 0 \quad \text{for } j = 1 \text{ to } \#\text{ of primitives} \\ 0 & \text{if } \Sigma_j C_{ij}(k) \leq 0 \quad \text{and } j \neq i, \end{cases}$$

$C_{ij} = (1/d_{ij}) \cdot \text{SIGN}(t - \mid f_i(k) - f_j(k) \mid)$, $k = 3, 10$,

s_i' = the complete features switch vector, derived from s_i under additional texture regularity constraints,

t is a threshold, and z is a large but arbitrary number.

Clustering is then performed using the features selected above. In the comparison performed in [13], this method gave the best performance, although it was considered computationally expensive.

TABLE 1
A Summary of the Feature Set Used by Abele

No.	Name
1	x-Coordinate
2	y-Coordinate
3	Brightness[a]
4	Directionality[a]
5	Orientation[a]
6	x-Regularity[a]
7	y-Regularity[a]
8	Area[a]
9	Roundness[a]
10	Brightness Backgr.[a]
11	Window-size x
12	Window-size y
13	Average Intensity
14	Standard Deviation
15	Contrast
16	Angular sec. mom.

[a] Features associated with texture primitives.

In [19], Dondes and Rosenfeld propose a pixel classification scheme based on mean gray level (calculated over a window centered on the pixel of interest) and the variation of the gray level within this window. This variation is termed "busyness," and is measured using either the "minimum total variation" (MTV), or the "median absolute difference" (MAD). For a 3 × 3 region,

$$\begin{matrix} a & b & c \\ d & e & f \\ g & h & i \end{matrix}$$

the MTV can be calculated as

$$\begin{aligned} \text{MTV} = \min[& | a-b | + | b-c | + | d-e | \\ & + | e-f | + | g-h | + | h-i | , \\ & | a-d | + | d-g | + | b-e | \\ & + | e-h | + | c-f | + | f-i |]. \end{aligned} \tag{5}$$

The MAD is the median of the absolute difference between all 12 pairs of horizontally or vertically adjacent pixels.

De Souza [20] proposes a method for detecting boundaries between regions using sliding statistical tests. One-dimensional profiles are examined using a sliding window. Five tests are considered, the most powerful of which is able to detect boundaries between textures with the same variance and average intensity.

A technique to predict the presence of textured regions using a pyramid structure is described by Lee in [21]. This method is based on the assumption that the averaging performed in constructing the pyramid will change a large textured region into a uniform region at the level in the pyramid where the averaging window is approximately the size of the texture primitives. The result of applying this algorithm is an image with connected textured regions extracted and untextured regions untouched.

Lowitz [22] proposes information extracted from local histograms as features for texture segmentation. In particular, the module and state of the histograms are suggested. For the pixel (m, n), centered in a window containing N pixels, and with r possible gray levels in the image, the module is

$$I_{MH}(m, n) = \sum_{i=1}^{r} \frac{n_i - N/r}{\sqrt{n_i(1 - n_i/N) + N(1 - 1/r)/r}}, \tag{6}$$

where n_i is the number of counts at the i^{th} gray level. The state is the index of the largest count of the local histogram.

A generalization of the run length concept is described by Shu *et al.* in [23]. The length of a run through the pixel (i, j) along the direction θ is defined as the maximum number of collinearly connected pixels with maximum and minimum gray levels differing by less than a specified threshold. Run lengths in horizontal, vertical, diagonal, and anti-diagonal ($\theta = 0°, 90°, 45°, -45°$) directions are used as features for segmentation.

In an attempt to discriminate between textures differing in high order statistics (greater than two), Sato and Ogata [24] propose a polynomial image transformation based on the self-organization method. The transformation is computed iteratively, with the goal of minimizing the sum of the variances over the two texture fields to be discriminated, while constraining the mean of the first field to be -1 and the mean of the second to be $+1$. The resulting transformation maps an image containing the two textures into an image with -1 over the first field and $+1$ over the second.

2.1.3. *Transform Domain Features*

An example of a segmentation method using transform domain features is that proposed by Xu and Fu in [25]. Scenes are initially segmented by use of multiple thresholds to reduce the number of gray levels in the image (and hence the dimensions of the co-occurrence matrices found in the next step). Segmentation is then performed using co-occurrence matrices and the split-and-merge algorithm, as recommended by Chen and Pavlidis [15]. Finally, the Walsh transform is used as a measure of coarseness to split regions that were over-merged in the previous step.

In [26], Jernigan and D'Astous propose entropies, calculated for subimages and over various regions of the subimage power spectrum, as a set of features. Based on between-to-within-class scatter, performance comparable to previous frequency domain features (energy summed over the same regions used to calculate the entropy) and to the contrast measure derived from gray level co-occurrence matrices are reported. Due to disappointing results obtained when using these entropy features to segment natural textures, however, the authors in [27] propose a set of features derived from the characteristics of power spectrum peaks and from the shape of the power spectrum. Features based on peak characteristics were peak strength, two-dimensional curvature, area, squared distance from the origin, and angular location. Frequency distribution shape features were elongation, spread, and "circularity" (the area of the distribution compared to the area of a circle having its radius equal to the major axis of the distribution). Applied to a set of natural textures, these features proved superior to summed energy features and co-occurrence matrix features.

2.1.4. *Other Features*

As would be expected, there are features used for segmentation that do not fall within the categories above. In

[28], Wechsler proposes planar random walks as a vehicle for texture segmentation. A planar random walk can be thought of as a particle moving in unit steps, in random directions. For four-connected pixels, the directions are up, down, left, and right. Walks are performed from the center of rectangular windows, distributed over the image. Let S_A, S_B, S_R, and S_L be the observed distributions of particle absorptions at the top, bottom, right, and left boundaries of the current region. Then a gradient can be defined as $g(m, \alpha)$, where

$$m = \sqrt{(S_R - S_L)^2 + (S_A - S_B)^2} \tag{7}$$

and

$$\alpha = \arctan \frac{S_A - S_B}{S_R - S_L}. \tag{8}$$

By forming a 2D histogram of the values for m and α over the image, clusters can be identified and labeled, yielding a segmentation.

A method based on curvilinear integration of gray levels along scan lines of different orientations is proposed by Barba and Ronsin in [29]. The scan lines start at the pixel of interest, and the length of the line required for the integral to reach a specified value is assigned to the pixel as a feature. This yields a feature vector of length k for each pixel, where k is the number of orientations selected.

In [30], Ashjari suggests the use of the singular value decomposition (SVD) to derive texture features. Windows of 32 × 32 pixels are decomposed to find their singular values, where for the window array $\boldsymbol{F}$, $\boldsymbol{F} = \mathbf{USV}^T$, and $\mathbf{S}$ is the diagonal matrix containing the singular values. The mean, variance, skewness, and kurtosis of the singular values for each window are computed and used as features. Using this method, textures that appear identical can be discriminated.

As a final instance of a novel texture feature, Kjell and Dyer [31] recommend the average separations of edges. Extended edge maps are computed from the image to be segmented, each with edges of a single orientation labeled with the average distance to the nearest extended edge of another selected orientation. This generates a map for each pair of edge orientations. These maps are then used in an overlapped pyramid structure to perform the segmentation.

2.2. Methods Using Unique Segmentation Techniques

2.2.1. *Region-Based Methods*

The MITES (model-driven, iterative texture segmentation) system, proposed by Davis and Mitiche in [32], combines selective feature smoothing with clustering. In supervised mode, statistical texture models supplied by the user are utilized in determining pixel classification. Each pixel is then replaced by an average of the pixels (within an analysis window centered on the pixel of interest) that are in the same class as the pixel replaced and that are contiguous neighbors. The classification and smoothing steps are repeated until the change in pixel labels becomes small. In the unsupervised mode, the classification step is replaced by clustering. Modifications to allow operations on edge-based (as opposed to pixel-based) texture features are described.

In [33], Lumia *et al.* propose a method using the facet model. The image of interest is first segmented using the facet model, yielding an image with each pixel assigned a region number. The regions are then numbered sequentially, and a region adjacency graph (RAG) is formed. For each region, a list of properties (features) are derived, including measures of region size, region shape, and gray level statistics within the region. Based on these features, the features of adjacent regions, and the features of textures from known images (acquired during a training phase), the regions are assigned texture categories.

Pietikäinen and Rosenfeld [34] propose a technique based on pyramid node linking. The pyramid structure is formed by producing images of decreasing resolution, with the high resolution image at the top of the pyramid. By linking regions (nodes) of one level with the most similar regions in neighboring levels, images can be segmented. This may be done either "top-down," in which case blocks judged homogeneous are linked to all of their subblocks, or "bottom-up," where subblocks similar to the parent block are linked to that block. A combination of these methods, with bottom-up linking used only on subblocks not merged in the top-down pass, was found most effective.

In [35, 36], Raafat and Wong describe a method directed by a resolution dependent texture information measure (I-measure). Since a region containing a boundary between textures contains more information than one that does not, an initial segmentation can be found by grouping blocks with low I-measure values. From these core regions, region growing takes places using a texture distance measure. Boundaries are then refined by breaking boundary blocks into four subblocks and merging each subblock with the region at the minimum texture distance.

A segmentation method based on a generalization of Hachimura–Kuwahara (H-K) edge preserving smoothing is proposed by Verbeek and de Jong [37]. An initial classification for each pixel is performed using overlapping windows. Each pixel is assigned the (known) texture whose feature vector is closest to that calculated over the pixels' window. Next, for each pixel, the four windows containing the pixel at one corner are examined. For each of these windows, the distance to the nearest known texture is calculated, and the closest class is assigned to the window. The pixel of interest is then assigned the texture

class of the window with the minimum distance (the window that was the closest match to the texture class assigned to it). In this way, a smoothing in feature space occurs, while preserving the boundaries between textures.

A modification of the split-and-merge algorithm is proposed by Doherty, Bjorklund, and Noga in [38]. The image to be segmented is first processed using the conventional split-and-merge, with mean gray scale value as the uniformity test. This is followed by a second merge pass, in which a predicate based on second-order statistics and relaxed mean gray scale uniformity is used. The result of this second pass is the elimination of overly split regions.

A final example of a region-based method is the diffusion region growing technique proposed by Reed, Wechsler, and Werman, in [39]. The region growing process proceeds as a modified random walk, where the probability of moving in a particular direction (and adding the pixel which is encountered to the region being grown) is determined by the similarity of the current and adjacent pixel characteristics. This method is able to grow several separate (but similar) regions simultaneously and is well suited to parallel implementation.

2.2.2. *Boundary-Based Methods*

An extension of the common edge detector techniques to the detection of texture boundaries is proposed by Grinaker in [40]. Instead of applying the edge detector (in this case the gradient) to the image itself, it is applied to a set of features derived from the image. This results in a set of "feature gradients," all of which may not be of the same discriminating capability or resolution. A feature gradient function (FGF) is defined as a sum of weighted, resolution-consistent feature gradients. Weights are assigned according to discriminating ability. Resolution is made consistent either by averaging high resolution features to be consistent with lower resolution features, rejecting lower resolution features, or estimating higher resolution versions of low resolution features.

A boundary-based method suggested for unsupervised texture segmentation is described by Wermser in [41]. A set of four masks, each with two subregions, are convolved with a set of features. The result is a set of eight new features for each of the original features. As shown in Fig. 2, the window subregions are vertically, anti-diagonally, horizontally, and diagonally opposed, respectively. By comparing the features from opposing subregions in each mask, a dissimilarity measure, s_n is determined. The amount, a, of the texture gradient $TG(a, d)$ is defined as

$$a = \max(s_n); n = 1, \ldots, 4. \quad (9)$$

The gradient direction is encoded as the number, n, of the mask yielding the maximum s_n. The best method for determining the dissimilarity measure was found to be the ratio of inter- and intra-class distance. Experiments are shown in which the segmentation is achieved by thresholding the amount of texture gradient and applying line thinning to the detected boundary.

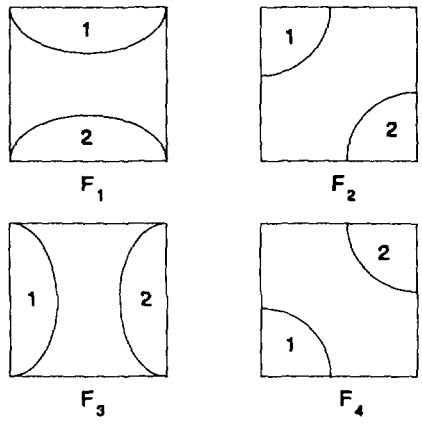

FIG. 2. Masks for texture gradient determination (from Wermser).

2.2.3. *Hybrid Methods*

In [42], Nazif and Levine describe a rule-based expert system combining both region and boundary information. Experiments comparing this system with the histogram splitting method of Ohlander [43] and the split-and-merge algorithm of Tanimoto and Pavlidis [44] are shown. Qualitatively, the segmentations achieved using the expert system compare very favorably to the other methods. A quantitative method of comparison is suggested by these authors in [45]. A comment on [42] regarding the implementation of the split-and-merge and the associated performance implications is made by Pavlidis in [46].

Finally, Spann and Wilson [47] propose a method, based on the quad-tree, that operates first on regions, then on the boundaries between regions. Quad-tree smoothing is performed, motivated by the fact that the variance of additive white Gaussian noise is reduced by a factor of two for each successive level of the tree. A level in the tree is then selected by the user (e.g., the level in the tree with the best signal to noise ratio). Clustering is performed at this level, yielding an initial segmentation. Class membership certainty is examined for each block, under the assumption that blocks containing boundaries will have a large measure of uncertainty. The boundary regions are refined by successive applications of smoothing, classification, and identification of boundary elements as the tree is traversed to its lowest (pixel) level.

3. MODEL-BASED METHODS

In this section we discuss two types of model-based methods, representative of the current state of the art in

this kind of system. A more complete survey of image models and a discussion of model-based segmentation is given by Kashyap in [48].

3.1. Fractal Models

Fractal functions have received a great deal of attention in recent years. Briefly, a fractal is a set for which the Hausdorff–Besicovich dimension (referred to as the fractal dimension) is strictly larger than the topological dimension.

Pentland [49] has found a high degree of correlation between fractal dimension and human estimates of roughness. Because of this correlation and the natural appearance of fractal-generated textures, Pentland has proposed fractal functions as texture models, and the fractal dimension as a feature for texture segmentation. The method used consists of four steps. First, the fractal dimension of each 8×8 block of pixels is estimated. Next, a histogram of the fractal dimensions is formed. This histogram is then broken at the "valleys" between modes. Finally, the image is segmented into regions belonging to each mode. The fractal dimension was estimated by examining the one-dimensional power spectrum along several directions and by averaging the results. That is, since the power spectrum $P(f)$ of a fractal Brownian function (the assumed texture model) is proportional to f^{-2H-1} and the fractal dimension is $D = T + (1 - H)$ (where T is the topological dimension), estimating the slope of the log power spectrum leads to an estimate of D. The segmentations produced by this method, applied to full gray-scale images, are relatively good. They have the added advantage that they are largely invariant to scaling of the image (since the fractal dimension of a Brownian function is scale invariant).

Rather than computing the slope of the (local) log power spectrum, alternative strategies can be followed to measure the fractal dimension. Medioni and Yasumoto [50] adopted a method which is based on gathering second-order difference or dipole statistics within a moving window, utilizing two distance vectors with different lengths.

Another alternative, explored by Peleg *et al.* in [51], is provided by the "blanket" method. Applying Mandelbrot's solution for the so-called "coastline of Britain problem" to the three-dimensional case, the image is covered by two surfaces, one above and one below, both with a specified distance ε to the gray values. The surface area equals the volume between the two surfaces divided by 2ε. This is done for various distances ε.

Related to the fractal dimension are space-filling curves, also referred to as self-similar or Hilbert curves. Nguyen and Quinqueton applied Peano scanning within a moving window in [52], measuring the fractal dimension on the Peano scan. A possible advantage of utilizing a Peano scan (within a window) instead of a normal horizontal or vertical raster scan is that the local neighborhood is better preserved. However, it is more difficult, if not impossible, to obtain specific anisotropic texture information.

It should be noted, as observed by Peleg *et al.* in [51], that textures in general are not fractals and at best can be considered so over only a limited range of scales. This being the case, it remains to be shown that textures can be discriminated based on fractal dimension, in the general case.

3.2. Stochastic Models and Decision-Theoretic Techniques

The application of stochastic methods to image modeling is an important and rapidly growing area. This is reflected in increasing application of these techniques to texture segmentation. In [53], Khotanzad and Bouarfa describe a parallel algorithm for segmentation using simultaneous autoregressive (SAR) random field models and multidimensional cluster analysis. Texture features are extracted by fitting two of these models to the image data in overlapping windows, resulting in six feature values per window. The sample mean and variance are used as additional features. The resulting feature vectors are histogrammed (in an eight-dimensional space) and local cluster peaks are detected. The validity of these peaks are tested by mapping the features back into the spatial domain and by evaluating their spatial spread. Clusters which map to pixel groupings which are not compact are considered invalid and are either merged with neighboring clusters or labeled as "noisy." The final clusters are assigned labels, mapped to the spatial domain, and noise cleaned to produce the final segmentation.

Khotanzad and Chen [54] describe an edge-based technique based on features derived from SAR random fields. The image of interest is partioned using overlapping windows, and the least squares estimates of the SAR model parameters are found for each window. Edges are enhanced in each of the resulting feature images via the Sobel operator. The enhanced images are then combined via a measure of "textural change," thresholded, and noise cleaned to produce an initial edge map. Because the SAR random field parameters are found over overlapping windows, the detected edges are as wide as the spacing between windows. To reduce this effect, the edges are then thinned to their "skeletons." It should be noted that the accuracy of the edges is determined by the window spacing, even though the edges are thinned to one pixel. As a result, significant deviation from the true texture boundary may result when the window spacing is large.

An alternative to heuristic segmentation approaches is to consider decision-theoretic methods, e.g., maximum likelihood (ML) or maximum a posteriori probability (MAP) estimation. These are often applied to the parame-

ters of stochastic texture models. We will briefly discuss a few region-based and boundary-based methods.

In [55], Huang proposes a two-state Markov model, applied to 1D profiles of the image of interest, to detect texture edges characterized by changes in first-order statistics. Each state is a texture, and the image gray values are modeled as the probabilistic outputs at the states. An iterative algorithm for computing the maximum-likelihood estimates of the state transition probabilities and output distributions is described, from which the state distribution at each pixel can be computed. An edge between textures is indicated by a step change in this distribution. Huang and Gong combine hidden Markov modeling with the Laws [6] texture energy measures in [56, 57]. In [56], the energy measures are used to classify the textures in the image before segmenting using the hidden Markov model. In [57], the segmentation is performed directly on the images resulting from the application of the energy measures.

A Gaussian random field model was incorporated into a split-and-merge algorithm by Bevington and Mersereau in [58]. Assuming Gaussian white noise distributions characterized by their mean and covariance, the image is first split using a maximum-likelihood boundary detection. Neighboring regions are then merged on the basis of a ranked statistical distance measure (e.g., Bhattacharyya) until a prescribed number of regions is obtained.

Stochastic image models based on the Gibbs distribution [59] are of great current interest. In [60], Derin and Elliot propose a hierarchical image model based on this distribution and use it for texture segmentation. They state the definition of the Gibbs distribution as follows. Consider the region L, shown in Fig. 3.

DEFINITION 1. A collection of subsets

$$\eta = \{\eta_{ij} : (i, j) \in L, \eta_{ij} \subseteq L\}$$

is a *neighborhood system* if and only if for each η_{ij} (the *neighborhood* of pixel (i, j))

1. $(i, j) \notin \eta_{ij}$, and
2. if $(k, l) \in \eta_{ij}$, then $(i, j) \in \eta_{kl}$ for any $(i, j) \in L$.

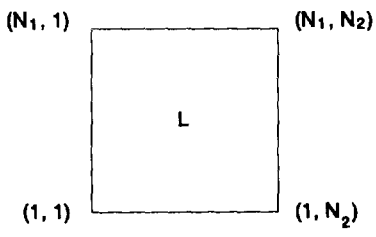

FIG. 3. The region of interest, L, in the definition of the Gibbs distribution.

DEFINITION 2. A *clique*, c, for the array L and neighborhood system η, is a subset of L, where

1. c consists of a single pixel, or
2. for $(i, j) \neq (k, l)$, $(i, j) \in c$ and $(k, l) \in c$ implies that $(i, j) \in \eta_{kl}$.

DEFINITION 3. A random field $X = \{X_{ij}\}$ defined on L has *Gibbs' distribution* or (equivalently) is a *Gibbs random field* with respect to the neighborhood system η if and only if its joint distribution has the form

$$P(X = x) = \frac{1}{Z} e^{-U(x)},$$

where

$$U(x) = \sum_{c \in C} V_c(x),$$

C = the collection of all cliques of (L, η),

$V_c(x)$ = the potential associated with the clique c,

$$Z = \sum_{x} e^{-U(x)}. \tag{10}$$

The hierarchical model proposed by Derin and Elliot has two levels. The high level Gibbs distribution models the regions in the image. The low level distributions model the textural properties of each region. Using this model, images are segmented based on the Gibbs distribution parameters via a dynamic programming method and MAP criterion. It should be noted that this segmentation method is currently applicable only to noise-free textured images consisting of known textures and with known high level Gibbs distribution parameters. An estimation procedure for the distribution parameters of textures is described, but it is only applicable to isolated samples of textures.

Kashyap and Eom [61, 62] examined the long correlation model for detecting texture boundaries. This model is inspired by fractional Gaussian noise, assuming that the correlation decreases with the lag k as k^{α}. Parameter estimation is performed on horizontal and vertical strips in the input image, and boundaries are detected using again a maximum-likelihood method. Small isolated boundary segments are removed by a boundary tracking procedure, and the remaining horizontal and vertical boundaries are combined in one output image.

The importance of the window size over which textures are examined was demonstrated by Chellappa and Chatterjee [63], who compared supervised texture classification on the basis of the Gaussian Markov random field (GMRF) model. Not unexpectedly, misclassification increases for smaller window sizes. Another supervised segmentation study was performed by Simchony and

Chellappa [64]. MAP estimation was applied to the parameters of the GMRF model, comparing stochastic relaxation and the ICM (deterministic iterated conditional mode) method as introduced by Besag [65]. The stochastic relaxation method appeared to give better results.

Application of the GMRF model to unsupervised texture segmentation is examined by Manjunath and Chellappa [66]. An initial segmentation is produced by dividing the image into nonoverlapping regions, estimating the GMRF parameters over these regions, then merging regions via clustering based on the normalized Euclidean distance between their parameter vectors. The parameters are then recomputed over the merged regions, and a finer segmentation is produced using pixel-based segmentation. Two approaches are examined for this final segmentation: approximation to the MAP estimate of the region labels and a method which minimizes misclassification error. Similar results are achieved for either approach.

Two algorithms for segmentation based on two-dimensional noncausal Markov random fields (MRFs) are discussed by Cohen and Cooper in [67]. The underlying image model is hierarchical, with separate MRF models for region structure and for the textures within the regions. The first algorithm uses a pyramid-like approach, assumes no a priori information about the true region structure, and seeks a maximum likelihood segmentation. The second is a relaxation algorithm, which seeks the MAP segmentation. In both cases, it is assumed that the textures in the image are from a fixed set of known textures.

The challenging problem of extracting model parameters in an unsupervised manner is addressed by Silverman and Cooper in [68]. Smooth regions of an image are modeled as polynomials with additive white noise, while textured regions are modeled as colored Gaussian Markov random fields with polynomial mean values. These models are first fit to the image data in nonoverlapping subblocks of the image. The subblocks are then merged, based on maximum likelihood or a more general Bayesian criterion. In the experiments shown, the resulting parameters are passed to the hierarchical algorithm described in [67], producing very accurate segmentations for some very difficult images.

A two-step segmentation procedure was applied in the supervised case by Fan and Cohen [69] and in the unsupervised case by Cohen and Fan [70]. In the first step, relatively large disjoint windows in an image are examined for homogeneity or heterogeneity, using the MRF model in combination with the ML method. The homogeneous windows are then combined on the basis of the statistics computed, which yields a coarse segmentation. In the second step the pixels in the windows judged to contain two or more texture classes are classified by means of a minimum distance criterion which maximizes the likelihood. This supervised classification results in a fine segmentation.

A similar technique, but incorporating a boundary-based method, was applied by Cohen *et al.* [71]. First, large homogeneous regions are detected by means of a pseudo-likelihood ratio test, resulting again in a coarse region-based segmentation. This is followed by a fine boundary detection by means of ML edge location estimation, thereby employing the class statistics established in the first step.

The results obtained by most of these methods, the boundary precision in particular, are quite good and underline the potential of decision-theoretic approaches for unsupervised image segmentation, but further tests with test images containing small regions and a more complex region geometry are required.

4. STRUCTURAL METHODS

Structural texture analysis and segmentation methods assume that textures are composed of well-defined texture elements. Since many textures violate this assumption, structural methods are of limited utility. Nevertheless, many of these approaches are interesting. In this section, we will discuss three such methods.

Jayaramamurthy [72] examines regular textures via the spatial-frequency domain. Given a texture primitive $h(x, y)$ and placement rule $c(x, y)$, the texture $t(x, y)$ can be defined as

$$t(x, y) = h(x, y) * c(x, y),$$

where

$$c(x, y) = \sum \delta(x - x_m, y - y_n), \tag{11}$$

and x_m and y_n are the coordinates of impulse functions (the centers of the texture primitives located in the associated regions of the images). In the spatial-frequency domain

$$T(u, v) = H(u, v) \cdot C(u, v), \tag{12}$$

so that

$$C(u, v) = T(u, v) \cdot H(u, v)^{-1}. \tag{13}$$

Thus, *given a description of a texture primitive* $h(x, y)$, we can derive a deconvolution filter $H(u, v)^{-1}$. Applying this filter to an image containing the texture of interest results in an array of impulses in the region of the image containing that texture. Each impulse is the center of a texture primitive.

In [73], Matsuyama, Saburi, and Nagao extract texture elements from a regular texture by region growing. To do this, it is assumed that a texture element is composed of connected pixels with similar gray levels. They then calculate the vectors between the elements. After estimat-

ing the locations of missing elements (by closely examining locations that the vectors predict as potential sites), the set of vectors is trimmed of redundancy to produce a relatively compact description of the placement of the elements. Segmentation is accomplished by moving templates of each texture element around the boundaries of their respective regions, as defined by the placement description.

Finally, Toriwaki, Yashima, and Yokoi [74] describe the adjacency of texture elements by extending the concepts of Voronoi neighbor, Gabriel neighbor, and relative neighbor (originally defined only for isolated points in continuous space) to connected components in a digitized image. Texture regions are extracted from binary images, for which the modified digital Voronoi diagram has been found, by thresholding the mean and variance of tile features (such as area). Texture boundaries are detected by thresholding the average edge length at each node in the image adjacency graph, under the assumption that edge lengths will be longer at the boundaries.

5. SPATIAL/SPATIAL-FREQUENCY TECHNIQUES

So far, we have considered texture segmentation methods as being either feature-based, model-based, or structural in nature. Approaches used in texture segmentation can also be grouped loosely into those based on statistical methods and those using spatial-frequency or spatial/spatial-frequency methods.

A number of statistical methods have been described in the previous sections. Spatial-frequency or spatial/spatial-frequency techniques described above include the operator-based and transform domain feature-based methods. Statistical methods have in the past proven superior to frequency domain techniques [75, 76]. This is due to the lack of locality in these early frequency analysis methods. Joint spatial/spatial-frequency techniques are inherently local in nature, and have characteristics that compare favorably with those of the statistical methods.

Joint spatial/spatial-frequency (s/sf) methods are based on image representations that indicate the frequency content in localized regions in the spatial domain. As such these methods overcome the shortcomings of the traditional Fourier-based techniques. Such methods are able to achieve high resolution in both the spatial and spatial-frequency domains and are consistent with recent theories on human vision. Specifically, there is a large and growing body of theory postulating local frequency analysis in the human visual system. It ranges in complexity from three or four frequency selective channels proposed by Crick, Marr, and Poggio [77] to a continuous spectrum of frequency analyzers. Such analyzers could be implemented through the use of 2D Gabor functions [78] and/or Gaussian-smoothed sectors [79]. Support for a spatial-frequency interpretation of human vision in predicting object recognition has been reported by Ginsburg [80]. Beck *et al.* [81] have shown correlation between the ability of humans to segment tripartite textured images and the outputs of a bank of 2D Gabor filters applied to the images.

The Wigner distribution (WD) is a s/sf representation which was first introduced (in its 1D form) in quantum mechanics, to characterize the positions and momenta of particles. The 2D pseudo-Wigner distribution (PWD), a discrete approximation of the continuous WD, is

$$PW(m, n, p, q) = 4 \sum_{k=-N_2+1}^{N_2-1} \sum_{l=-N_1+1}^{N_1-1} h_{N_1,N_2}(k, l) \times \sum_{r=-M_2+1}^{M_2-1} \sum_{s=-M_1+1}^{M_1-1} g_{M_1,M_2}(r, s) f(m + r + k, n + s + l) \times f^*(m + r - k, n + s - l) e^{-j(2\pi kp/P + 2\pi lq/Q)} \quad (14)$$

where $p = 0, \pm 1, \ldots, \pm (N_2 - 1)$, $q = 0, \pm 1, \ldots, \pm (N_1 - 1)$, $P = 2N_2 - 1$, $Q = 2N_1 - 1$, m and n are integers, and the functions $h_{N_1,N_2}(k, l)$ and $g_{M_1,N_2}(r, s)$ are window functions. The 2D PWD was first used for texture segmentation by Reed and Wechsler [82]. Their technique was refined and extended to consider perceptual (Gestalt) grouping effects in [83]. This aspect was further examined in [84]. It was found that in addition to being useful for texture segmentation, object groupings consistent with preattentive grouping as observed in humans could be obtained using the PWD.

A key issue in comparing joint spatial/spatial-frequency representations, especially for use in segmentation, is the resolution that can be attained (simultaneously) in the two domains. The WD has the highest joint resolution of any such representation. Although real-valued, it also encodes phase information. Because the WD and PWD are bilinear, however, troublesome crossterms may occur for complex textures. Furthermore, as is typical for s/sf representations, the PWD yields a set of potential texture features of very large dimensionality. Selecting between these features is difficult, in general. The approach taken in [82–84] was to determine the high energy frequency components in the PWD of the image to be segmented and to select a small set of these components ("frequency planes") as features. For complex images, this approach may not be suitable.

Turner showed that the Gabor power spectrum captures important information for a wide variety of textures [85]. Because he could not show all filter results, he decided to sum the filter responses over different filter subsets. This solution, which is based on prior texture information, connects to one of the basic problems related to the use of Gabor filter sets: their dimensionality. If small changes in texture frequency and orientation have to be captured, the number of filters required will be large. Research effort

therefore seems to concentrate on methods which combine or code the filter results. We will mention a few approaches.

Jain and Farrokhnia [86] used even-symmetric Gabor filters, i.e., the real part only, which often results in characteristically striped responses. These responses are input to a sigmoidal nonlinearity, and the average absolute deviation from the mean in a moving window is computed to measure the local energy. Filter selection is based on ranking the integrated power in the frequency bands, analysing the global power spectrum, and taking the filter subset for which the summed power is a given fraction of the total power (95%). Starting with an initial set of 20 filters, 11 to 13 filters were required to segment simple Brodatz patch images. In the case of a mosaic of 16 textures, all 20 filters, supplemented by pixel coordinate information, were required to achieve acceptable results.

Bovik, Clark, and Geisler [87] adopted a simple peak finding scheme applied to the global power spectrum in order to select the filters. Feature selection was based on taking the maximum filter response at any position in the image. They used only two filters, which is justified by the extreme simplicity of their test images (containing only two textures).

A recent development is the computation of higher-order Gabor features. Considering the local Gabor power spectrum as a two-dimensional array in log-polar frequency coordinates, du Buf [88] applied a least-squares approximation using a separable Gaussian with only five free parameters, thereby reducing the number of features from 30 to five. The resulting parameters describe the shape of the local power spectrum and are interpretable in terms of visually relevant texture attributes (like fine/coarse, isotropic/anisotropic). Another way to describe the shape of the local power spectrum is to use central moments. Real and complex moments are compared by Bigun and du Buf in [89, 90]. Real moments provide a "blind" mathematical description, but complex moments are shown to provide measures of the n-fold symmetry; i.e., they enable a discrimination between linear, rectangular, and hexagonal geometric structures at different frequency scales.

A fundamental problem of these higher-order Gabor features is the fact that elongated regions are often detected on texture boundaries if a region-based segmentation algorithm is applied (Spann and Wilson's [47] quadtree method has been applied in the two studies above). This effect is due to the sensitivity of some parameters to the mixture of two power spectra at a boundary. This effect can be circumvented by a boundary-based approach in Gabor space. A simple polar-complex boundary detector, the local spectral dissimilarity estimate, was defined by du Buf in [91]. The magnitude of this estimate gives the probability of a nearby boundary, while the argument gives the direction in which this boundary can be found. Subsequent thresholding and region growing gave good results if the textures were characterized by distinct peaks in the local power spectrum, even if the textures changed gradually.

All techniques described above are based exclusively on the Gabor power spectrum. For highly structured textures, the phase spectrum carries important information as well. The extraction of useful local phase information is hampered by the classical two-dimensional phase unwrapping problem. This can be circumvented by computing the phase gradient [87]. Other techniques, explored in [92, 93] are based on global or local phase demodulation, as well as the direct use of the discontinuities and isolated zero points in a phase image. Unfortunately, it has been shown that bandpass noise, and a small amount of jitter of texture's structural elements in particular, leads to a drastic reduction in the quality of local phase features.

6. CONCLUDING REMARKS

In this paper, we have briefly examined a number of recent texture segmentation techniques, with a primary focus on those which have potential for unsupervised applications. Even with this relatively restricted emphasis, however, there is a vast body of literature to be considered. There are many different techniques in existence, and each year many new or improved approaches are reported. To further complicate the situation, these methods may have distinct application areas; e.g., some model-based methods are suitable only for stochastic textures. Other methods, such as those based on the use of certain transforms or filter banks, may have promise for addressing both stochastic and structural textures.

A rigorous quantitative comparison of these various methods presents a demanding and time consuming task. Among the few existing papers which attempt such comparisons (although of a somewhat more limited breadth) are [76, 6, 94–96]. A fundamental question which must be addressed is how to compare performance quantitatively. Typical evaluation criteria may be based on either direct feature statistics (some measure of class separation) or on boundary accuracy after segmentation. It was shown in [96], for example, that the Bhattacharya distance is not a suitable measure for this application, due to the nonlinear behavior of the segmentation process. A weighted combination of boundary accuracy and the number of true regions identified may be useful. However, this approach is complicated by the complex region geometry encountered in most images.

Once a technique for quantitative comparison is determined, extensive tests are required. Ideally, a standard set of test images should be used, possibly including synthetic textures, Brodatz (natural) textures, and textures from aerial and satellite imagery, with varying geometrical region complexity. A comprehensive quantitative analysis

of this scope, despite its undeniable value, has yet to be undertaken.

REFERENCES

1. R. M. Haralick, Statistical and structural approaches to texture, *Proc. IEEE* **67**, 1979, 786–804.
2. L. S. Davis, Image texture analysis techniques—A survey, in *Digital Image Processing* (J. C. Simon and R. M. Haralick, Eds.), pp. 189–201, Reidel, Dordrecht, 1981.
3. L. Van Gool, P. Dewaele, and A. Oosterlinck, Texture analysis anno 1983, *Comput. Vision Graphics Image Process.* **29**, 1985, 336–357.
4. R. M. Haralick, Image segmentation survey, in *Fundamentals in Computer Vision* (O. D. Faugeras, Ed.), pp. 209–224, Cambridge Univ. Press, Cambridge, 1983.
5. R. M. Haralick and L. M. Shapiro, Image segmentation techniques, *Comput. Vision Graphics Image Process.* **29**, 1985, 100–132.
6. K. I. Laws, *Textured Image Segmentation*, Technical Report USCIPI Report 940, Dept. of Elec. Eng., Image Processing Institute, Univ. of Southern California, Los Angeles, January 1980.
7. R. W. Conners, M. M. Trivedi, and C. A. Harlow, Segmentation of a high-resolution urban scene using texture operators, *Comput. Vision Graphics Image Process.* **25**, 1984, 273–310.
8. R. M. Haralick, K. Shanmugam, and I. Dinstein, Textural features for image classification, *IEEE Trans. Systems Man Cybernet.* **3**(1), 1973, 610–621.
9. I. Dinstein, A. C. Fong, L. M. Ni, and K. Y. Wong, Fast discrimination between homogeneous and textured regions, in *Proceedings, 7th International Conference on Pattern Recognition, Montreal, Canada, July 30–August 2, 1984*, pp. 361–363.
10. M. Unser, Local linear transforms for texture measurements, *Signal Process.* **11**, 1986, 61–79.
11. R. Wang, A. R. Hanson, and E. M. Riseman, Texture analysis based on local standard deviation of intensity, *IEEE Computer Society Conference on Computer Vision and Pattern Recognition, Miami Beach, Florida, June 22–26, 1986*, pp. 482–488.
12. G. H. Granlund, Description of texture using the general operator approach, in *Proceedings, 5th International Conference on Pattern Recognition, Miami Beach, Florida, December 1–4, 1980*, pp. 776–779.
13. D. Wermser and N. Lissel, Comparison of algorithms for unsupervised segmentation of images by the use of texture information, in *Proceedings of the 2nd European Signal Processing Conference, Erlangen, West Germany, September 12–16, 1983*, pp. 287–290.
14. L. W. Abele, Feature selection by space invariant comparison with applications to the segmentation of textured pictures, in *Proceedings of the 5th International Conference on Pattern Recognition, Miami Beach, Florida, December 1–4, 1980*, pp. 535–539.
15. P. C. Chen and T. Pavlidis, Segmentation by texture using a co-occurence matrix and a split-and-merge algorithm, *Comput. Graphics Image Process.* **10**, 1979, 172–182.
16. H. Knutsson and G. H. Granlund, Texture analysis using two-dimensional quadrature filters, in *IEEE Workshop CAPAIDM, Pasadena, CA, 1983*, pp. 206–213.
17. J. Bigun, Frequency and orientation selective texture measures using linear symmetry and Laplacian pyramid, in *Proceedings Visual Communications and Image Processing, Lausanne, Switzerland, October 2–4, 1990*, pp. 1319–1331.
18. H. Tamura, S. Mori, and T. Yamawaki, Texture features corresponding to visual perception, *IEEE Trans. Systems Man Cybernet.* **8**, 1978, 460–473.
19. P. A. Dondes and A. Rosenfeld, Pixel classification based on gray level and local "busyness," *IEEE Trans. Pattern Anal. Mach. Intell.* **4**(1), 1982, 79–84.
20. P. de Souza, Edge detection using sliding statistical tests, *Comput. Vision Graphics Image Process.* **23**, 1983, 1–14.
21. H. Y. Lee, Extraction of textured regions in aerial imagery, in *Image Understanding, Proceedings, Workshop, Arlington, VA, June 23, 1983* (L. S. Baumann, Ed.), pp. 298–303, Science Appl., McLean, VA, 1983.
22. G. E. Lowitz, Can a local histogram really map texture information?, *Pattern Recognit.* **16**(2), 1983, 141–147.
23. D. B. C. Shu, Y. N. Sun, C. C. Li, and J. F. Mancuso, Run length based image segmentation schemes, in *Proceedings, IEEE Computer Society Conference on Computer Vision and Pattern Recognition, Washington, DC, June 19–23, 1983*, pp. 154–156.
24. M. Sato and M. Ogata, Texture analysis by the self-organization method, in *Proceedings, 7th International Conference on Pattern Recognition, Montreal, Canada, July 30–August 2, 1984*, pp. 1213–1215.
25. G. Y. Xu and K. S. Fu, Natural scene segmentation based on multiple threshold and texture measurement, in *Proceedings, 7th International Conference on Pattern Recognition, Montreal, Canada, July 30–August 2, 1984*, pp. 1111–1113.
26. M. E. Jernigan and F. D'Astous, Entropy-based texture analysis in the spatial frequency domain, *IEEE Trans. Pattern Anal. Mach. Intell.* **6**(2), 1984, 237–243.
27. F. D'Astous and M. E. Jernigan, Texture discrimination based on detailed measures of the power spectrum, in *Proceedings, 7th International Conference on Pattern Recognition, Montreal, Canada, July 30–August 2, 1984*, pp. 83–86.
28. H. Wechsler, Taxonomy and segmentation of textured images, in *Proceedings, 5th International Conference on Pattern Recognition, Miami Beach, Florida, December 1–4, 1980*, pp. 532–534.
29. D. Barba and J. Ronsin, New method in texture analysis in the context of image segmentation, in *Proceedings, 2nd European Signal Processing Conference, Erlangen, West Germany, September 12–16, 1983*, pp. 283–286.
30. B. Ashjari, Computer detection and identification of a visually indiscernable texture mixture, in *Proceedings, IEEE Computer Society Conference on Computer Vision and Pattern Recognition, San Francisco, CA, June 19–23, 1985*, pp. 172–174.
31. B. P. Kjell and C. R. Dyer, Segmentation of textured images, in *Proceedings, IEEE Computer Society Conference on Computer Vision and Pattern Recognition, Miami Beach, Florida, June 22–26, 1986*, pp. 476–481.
32. L. S. Davis and A. Mitiche, Mites: A model-driven, iterative texture segmentation algorithm, *Comput. Graphics Image Process.* **19**, 1982, 95–110.
33. R. Lumia, R. M. Haralick, O. Zuniga, L. Shapiro, T. C. Pong, and F. P. Wang, Texture analysis of aerial photographs, *Pattern Recognit.* **16**(1), 1983, 39–46.
34. M. Pietikainen and A. Rosenfeld, Image segmentation by texture using pyramid node linking, *IEEE Trans. Systems Man Cybernet.* **11**(12), 1981, 822–825.
35. H. M. Raafat and A. K. C. Wong, Texture information directed algorithm for biological image segmentation and classification, in *Proceedings, International Conference on Cybernetics and Society, Cambridge, Massachusetts, October 8–10, 1980*, pp. 1003–1008.
36. H. M. Raafat and A. K. C. Wong, Texture-based image segmentation, in *Proceedings, IEEE Computer Society Conference on Computer Vision and Pattern Recognition, Miami Beach, Florida, June 22–26, 1986*, pp. 469–475.

37. P. W. Verbeek and D. J. de Jong, Edge preserving texture analysis, in *Proceedings, 7th International Conference on Pattern Recognition, Montreal, Canada, July 30–August 2, 1984*, pp. 1030–1032.
38. M. F. Doherty, C. M. Bjorklund, and M. T. Noga, Split-merge-merge: An enhanced segmentation capability, in *Proceedings, IEEE Computer Society Conference on Computer Vision and Pattern Recognition, Miami Beach, Florida, June 22–26, 1986*, pp. 325–330.
39. T. R. Reed, H. Wechsler, and M. Werman, Texture segmentation using a diffusion region growing technique, *Pattern Recognit.* **23**(9), 1990, 953–960.
40. S. Grinaker, Edge based segmentation and texture separation, in *Proceedings, 5th International Conference on Pattern Recognition, Miami Beach, Florida, December 1–4, 1980*, pp. 554–557.
41. D. Wermser, Unsupervised segmentation by use of a texture gradient, in *Proceedings, 7th International Conference on Pattern Recognition, Montreal, Canada, July 30–August 2, 1984*, pp. 1114–1116.
42. A. M. Nazif and M. D. Levine, Low level image segmentation: An expert system, *IEEE Trans. Pattern Anal. Mach. Intell.* **6**(5), 1984, 555–577.
43. R. Ohlander, *Analysis of Natural Scenes*, Ph.D. thesis, Carnegie-Mellon University, Pittsburgh, PA, April 1975.
44. S. Tanimoto and T. Pavlidis, A hierarchical data structure for picture processing, *Comput. Graphics Image Process.* **4**, 1975, 104–119.
45. M. D. Levine and A. M. Nazif, Dynamic measurement of computer generated image segmentations, *IEEE Trans. Pattern Anal. Mach. Intell.* **7**(2) 1985, 155–164.
46. T. Pavlidis, Comments on "low level segmentation: an expert system," *IEEE Trans. Pattern Anal. Mach. Intell.* **8**(5), 1986, 675–676.
47. M. Spann and R. Wilson, A quad-tree approach to image segmentation which combines statistical and spatial information, *Pattern Recognit.* **18**(3/4), 1985, 257–269.
48. R. L. Kashyap, Image models, in *Handbook of Pattern Recognition and Image Processing* (T. Y. Young and K. S. Fu, Ed.) Chap. 12, pp. 281–310, Academic Press, New York, 1986.
49. A. P. Pentland, Fractal-based description of natural scenes, *IEEE Trans. Pattern Anal. Mach. Intell.* **6**(6), 1984, 661–674.
50. G. G. Medioni and Y. Yasumoto, A note on using the fractal dimension for segmentation, in *IEEE Computer Vision Workshop, Annapolis, MD, 1984*, pp. 25–30.
51. S. Peleg, J. Naor, R. Hartley, and D. Avnir, Multiple resolution texture analysis and classification, *IEEE Trans. Pattern Anal. Mach. Intell.* **6**, 1984, 518–523.
52. P. T. Nguyen and J. Quinqueton, Space filling curves and texture analysis, in *Proceedings, 6th Int. Conf. on Pattern Recognition, Munich, Germany, 1982*, pp. 282–285.
53. A. Khotanzad and A. Bouarfa, A parallel, non-parametric, non-iterative clustering algorithm with application to image segmentation, in *Proceedings, 22nd Asilomar Conference on Signals, Systems, and Computers, IEEE Computer Society, Pacific Grove, CA, October 31–November 2, 1988* (R. R. Chen, Ed.), pp. 305–309.
54. A. Khotanzad and J. Chen, Unsupervised segmentation of textured images by edge detection in multidimensional features, *IEEE Trans. Pattern Anal. Mach. Intell.* **11**(4), 1989, 414–421.
55. N. K. Huang, Markov model for image segmentation, in *Proceedings, 22nd Allerton Conference on Communication, Control, and Computing, Montecello, IL, October 3–5, 1984*, pp. 775–781.
56. N. K. Huang and X. Gong, Textured image recognition using the hidden Markov model, in *Proceedings* of the *International Conference on Acoustics, Speech and Signal Processing-88, New York, NY, April 11–14, 1988*, pp. 1128–1131.
57. X. Gong and N. K. Huang, Texture segmentation using iterative estimate of energy states, in *Proceedings, 9th International Conference on Pattern Recognition, Rome, Italy, November 14–17, 1988*, pp. 51–55.
58. J. E. Bevington and R. M. Mersereau, A random field model based algorithm for textured image segmentation, in *Proceedings, 3rd European Signal Processing Conference, The Hague, The Netherlands, September 2–5, 1986*, pp. 909–912.
59. S. Geman and D. Geman, Stochastic relaxation, Gibbs distributions, and Bayesian restoration of images, *IEEE Trans. Pattern Anal. Mach. Intell.* **6**(6), 1984, 721–741.
60. H. Derin and H. Elliot, Modeling and segmentation of noisy and textured images using Gibbs random fields, *IEEE Trans. Pattern Anal. Mach. Intell.* **9**(1), 1987, 39–55.
61. R. L. Kashyap and K. Eom, Texture boundary detection based on long correlation model, in *Proceedings, 23rd Allerton Conf. on Communication, Control, and Computing, Monticello, Illinois, October 2–4, 1985*, pp. 314–323.
62. R. L. Kashyap and K. B. Eom, Texture boundary detection based on the long correlation model, *IEEE Trans. Pattern Anal. Mach. Intell.* **11**, 1989, 58–67.
63. R. Chellappa and S. Chatterjee, Classification of textures using Gaussian Markov random fields, *IEEE Trans. Acoust. Speech Signal Process.* **33**(4), 1985, 959–963.
64. T. Simchony and R. Chellappa, Stochastic and deterministic algorithms for MAP texture segmentation, in *Proceedings, IEEE Int. Conf. on Acoustics, Speech, and Signal Processing, New York, NY, April 11–14, 1988*, pp. 1120–1123.
65. J. Besag, On the statistical analysis of dirty pictures, *J. R. Statist. Soc. B* **48**, 1986, 259–302.
66. B. S. Manjunath and R. Chellappa, Unsupervised texture segmentation using Markov random field models, *IEEE Trans. Pattern Anal. Mach. Intell.* **13**(5), 1991, 478–482.
67. F. S. Cohen and D. B. Cooper, Simple parallel hierarchical and relaxation algorithms for segmenting noncausal Markovian random fields, *IEEE Trans. Pattern Anal. Mach. Intell.* **9**(2), 1987, 195–219.
68. J. Silverman and D. Cooper, Bayesian clustering for unsupervised estimation of surfaces and texture models, *IEEE Trans. Pattern Anal. Mach. Intell.* **10**(4), 1988, 482–495.
69. Z. Fan and F. S. Cohen, Textured image segmentation as a multiple hypothesis test, *IEEE Trans. Circuits Systems* **35**(6), 1988, 691–702.
70. F. S. Cohen and Z. Fan, Maximum likelihood unsupervised textured image segmentation, *Computer Vision Graphics Image Process. Graph. Models Image Process.* **54**(3), 1992, 239–251.
71. F. Cohen, Y. Liu, and Z. Fan, Detection and localization of edges in textured images modeled by gaussian markov random fields, in *13th GRETSI Symposium on Signal and Image Processing, Juans les Pins, France, September 16–20, 1991*, pp. 1161–1164.
72. S. N. Jayaramamurthy, Texture discrimination using digital deconvolution filters, in *Proceedings, 5th International Conference on Pattern Recognition, Miami Beach, Florida, December 1–4, 1980*, pp. 1184–1186.
73. T. Matsuyama, K. Saburi, and M. Nagao, A structural analyzer for regularly arranged textures, *Comput. Graphics Image Process.* **18**, 1982, 259–278.
74. J. Toriwaki, Y. Yashima, and S. Yokoi, Adjacency graphs on a digitized figure set and their applications to texture analysis, in *Proceedings, 7th International Conference on Pattern Recognition, Montreal, Canada, July 30–August 2, 1984*, pp. 1216–1218.
75. R. W. Connors and C. A. Harlow, A theoretical comparison of texture algorithms, *IEEE Trans. Pattern Anal. Mach. Intell.* **2**(3), 1980, 204–222.

76. J. S. Weszka, C. R. Dyer, and A. Rosenfeld, A comparison study of texture measures for terrain classification, *IEEE Trans. Systems Man Cybernet.* **6**(4), 1976, 269–286.

77. F. H. C. Crick, D. C. Marr, and T. Poggio, *An Information Processing Approach to Understanding the Visual Cortex*, A. I. Memo 557, MIT, April 1980.

78. J. G. Daugman, Uncertainty relation for resolution in space, spatial frequency, and orientation optimized by two-dimensional visual cortical filters, *J. Opt. Soc. Am. A* **2**(7), 1985, 1160–1169.

79. A. B. Watson, The cortex transform: Rapid computation of simulated neural images, *Comput. Vision Graphics Image Process.* **39**, 1987, 311–327.

80. A. P. Ginsburg, Specifying relevant spatial information for image evaluation and display design: An explanation of how we see certain objects, *Proc. SID* **21**(3), 1980, 219–227.

81. J. Beck, A. Sutter, and R. Ivry, Spatial frequency channels and perceptual grouping in texture segregation, *Comput. Vision Graphics Image Process.* **37**, 1987, 299–325.

82. T. R. Reed and H. Wechsler, Tracking of non-stationarities for texture fields, *Signal Process.* **14**(1), 1988, 95–102.

83. T. R. Reed and H. Wechsler, Segmentation of textured images and Gestalt organization using spatial/spatial-frequency representations, *IEEE Trans. Pattern Anal. Mach. Intell.* **12**(1), 1990, 1–12.

84. T. R. Reed and H. Wechsler, Spatial/spatial-frequency representations for image segmentation and grouping, *Image Vision Comput.* **9**(3), 1991, 175–193.

85. M. R. Turner, Texture discrimination by Gabor functions, *Biol. Cybernet.* **55**, 1986, 71–82.

86. A. K. Jain and F. Farrokhnia, Unsupervised texture segmentation using Gabor filters, *Pattern Recognit.* **24**(12), 1991, 1167–1186.

87. A. C. Bovik, M. Clark, and W. S. Geisler, Multichannel texture analysis using localized spatial filters, *IEEE Trans. Pattern Anal. Mach. Intell.* **12**, 1990, 55–73.

88. J. M. H. du Buf, Abstract processes in texture discrimination, *Spatial Vision* **6**(3), 1992, 221–242.

89. J. Bigun and J. M. H. du Buf, Texture segmentation by real and complex moments of the Gabor power spectrum, in *Progress in Image Analysis and Processing II* (V. Cantoni *et al.*, Eds.), pp. 191–198, World Scientific, Singapore, 1992.

90. J. Bigun and J. M. H. du Buf, N-folded symmetries by complex moments in Gabor space and their application to texture segmentation, *IEEE Trans. Pattern Anal. Mach. Intell.*, in press.

91. J. M. H. du Buf, Towards unsupervised texture segmentation using Gabor spectral decomposition, in *Progress in Image Analysis and Processing* (V. Cantoni, L. P. Cordella, S. Levialdi, and G. Sanniti di Baja, Ed.), pp. 65–72, World Scientific, Singapore, 1990.

92. J. M. H. du Buf, Gabor phase in texture discrimination, *Signal Process.* **21**, 1990, 221–240.

93. J. M. H. du Buf and P. Heitkamper, Texture features based on Gabor phase, *Signal Process.* **23**, 1991, 227–244.

94. C. H. Chen, On the statistical image segmentation techniques, in *Proceedings, IEEE Computer Society Conference on Pattern Recognition and Image Processing, Dallas, Texas, August 3–5, 1981*, pp. 262–266.

95. M. Pietikainen, *Image Texture Analysis and Segmentation*, Ph.D. thesis, University of Oulu, Finland, 1982.

96. J. M. H. du Buf, M. Kardan, and M. Spann, Texture feature performance for image segmentation, *Pattern Recognit.* **23**(3/4), 1990, 291–309.